Taylor & Francis
Taylor & Francis Group

Drug Development and Industrial Pharmacy

ISSN: 0363-9045 (Print) 1520-5762 (Online) Journal homepage: https://www.tandfonline.com/loi/iddi20

Coprocessing of cellulose II with amorphous silicon dioxide: effect of silicification on the powder and tableting properties

John Rojas & Vijay Kumar

To cite this article: John Rojas & Vijay Kumar (2012) Coprocessing of cellulose II with amorphous silicon dioxide: effect of silicification on the powder and tableting properties, Drug Development and Industrial Pharmacy, 38:2, 209-226, DOI: 10.3109/03639045.2011.597400

To link to this article: https://doi.org/10.3109/03639045.2011.597400

Published online: 16 Nov 2011.

Drug Development and Industrial Pharmacy, 2012; 38(2): 209–226

ISSN 0363-9045 print/ISSN 1520-5762 online
DOI: 10.3109/03639045.2011.597400

informa
healthcare

RESEARCH ARTICLE

Coprocessing of cellulose II with amorphous silicon dioxide: effect of silicification on the powder and tableting properties

John Rojas and Vijay Kumar

Division of Pharmaceutics and Translational Therapeutics, College of Pharmacy, The University of Iowa, Iowa City, Iowa, USA

Abstract

Aim: In recent years, coprocessing has been the most successful approach to improve and correct the functionality of excipients. The aim of this study is to coprocessed cellulose II with SiO_2 and to evaluate the resulting powder and tableting properties.

Methods: Novel cellulose II:SiO_2 (98:2, 95:5, 90:10 and 80:20 w/w ratios) composites were produced by spray drying, wet granulation and spheronization techniques and the resulting powder and tableting properties were assessed.

Results: Cellulose II:SiO_2 composites produced by spray- drying exhibited spherical/oblongate shape, narrow distribution and mean diameter from 51 to 75 μm. The composites produced by wet granulation had larger distribution, granular shape and a mean diameter from 105 to 129 μm. The spheronized composites showed the highest size (from 148 to 450 μm) and round shape. Bulk and tap densities and flow were reduced as the silicification level increased in the spray dried and wet granulated materials. Likewise, silicification increased the true density, porosity and surface roughness of these materials. Water sorption decreased only at silicification level of 20% being comparable to the ones shown by Prosolv® samples. Contact angles of all cellulose II materials were lower than those of cellulose I except for Celphere203 indicating better wettability. A 5% and 10% silicification levels rendered the strongest compacts for the spray dried and wet granulated materials, respectively. Silicification did not affect the fast disintegration properties of MCCII.

Conclusions: Coprocessing proved to be useful tool to modify the powder and tableting properties of cellulose II.

Keywords: Coprocessed excipient, direct compression, silicon dioxide, cellulose II

Introduction

For many years, not a single new chemical excipient has been introduced into the market. Excipients have only been developed in response to market demands due to the relatively high cost involved with discovery, development and toxicology tests required for new excipients. There is a growing pressure on formulators to search for new excipients quickly, with no scaling up, manufacturing and environmental costs to achieve the desired set of functionalities. The growing popularity of the direct compression process demands for an ideal excipient, which can substitute two or more ingredients in a formulation avoiding the need for disintegrant, lubricant, glidant, etc[1].

In the past three decades excipients have been physically engineered for developing new grades such as pregelatinized starch, Avicel PH101, Avicel PH200, spray dried lactose, etc[2]. New grades of existing excipients are created by modifying the fundamental properties such as morphology, particle size, shape, surface area, porosity and density, which are reflected in the improved derived properties such as flowability, compressibility, compactibility, dilution, disintegration and lubrication potentials[3,4]. However, when one attribute is improved, another is compromised, i.e., flow of Avicel PH200 is improved at the expense of its compactibility and viceversa for Avicel PH101[5]. In order to overcome that problem in recent years coprocessing of two or three excipients have been undertaken. In this technique excipients interact at the particle level providing a synergy of functionality as well as masking

Address for Correspondence: John Rojas, Division of Pharmaceutics and Translational Therapeutics, College of Pharmacy, The University of Iowa, Iowa City, S213 Grand Avenue, Iowa 52242, USA. Tel.: 319 335–8836. Fax: (319) 335–9349. E-mail: jhon-rojascamargo@uiowa.edu

(Received 07 March 2011; revised 30 May 2011; accepted 13 June 2011)

of the undesirable properties of the individual components[6]. The resulting excipient has superior properties compared to the simple physical blending of their components[7]. The products so formed are physically modified in a way they do not lose their chemical structure and stability. This means that excipients maintain their independent chemical properties[3]. The randomized embedding of the components in the particles minimizes their anisotropic behavior. Particles of one material can be incorporated either on the surface or within the core of the companion material by spray-drying, wet granulation, spheronization, co-milling, co-crystallization, etc.

Recently, cellulose II powders, prepared from hydrocellulose and commercial MCCs by treatment with sodium hydroxide solutions at room temperature have been found to be useful as a multifunctional direct compression excipient[8]. In general, cellulose II powders show lower crystallinity and higher bulk and tap densities, compared to the starting cellulose I counterpart. They are less ductile and their compacts, irrespective of the compression force used to prepare them, disintegrate rapidly[9–13]. In this study, for the first time coprocessing of cellulose II with SiO_2 by spray-drying, wet granulation and spheronization was undertaken and the resulting changes of the powder properties with silicification and processing were revealed. Amorphous silicon dioxide was selected as the coprocessing agent because it is safe, when ingested, passes unchanged through the GI tract and excreted in the feces. It also has a high surface area (200 ± 15 m^2/g) and shows low water solubility (0.012 g/100 g). As supplied, it contains low moisture content (~1%). It serves as antistatic and it has superior glidant properties than magnesium stearate and talc. The study of cellulose II with enhanced physicochemical and mechanical properties through coprocessing represents not only an alternative but also an attractive research area. The increasing market is continuously demanding for new, improved or less expensive excipients.

Materials and methods

Materials

Cotton linter sheets (grade R270) were obtained from Southern Cellulose Products, Inc. (Chattanooga, TN). Hydrochloric acid and sodium hydroxide were purchased from Fisher Scientific (Fair Lawn, NJ). Amorphous silicon dioxide (Cab-o-Sil M5, lot I107) was obtained from Eager polymers (Chicago, IL). Prosolv® SMCC50 (lot XCSD9D661X) and Prosolv® SMCC90 (lot XCSD5B61X) were received from JRS Pharma (Patterson, NY). Celphere®203 (Lot 26J10) was obtained from Asahi Kasei Chemical (Tokio, JP).

Preparation of cellulose II powder (MCCII)

Cotton linter was soaked in 7.5 N NaOH for 72 h (cellulose:NaOH ratio 1:6, w/v) with periodic stirring at room temperature. The NaOH-treated cotton linter strips were collected by filtration and washed with distilled water until pH ranging between 5 and 7. Approximately 280 g of the dry material was then transferred to a five-liter reactor and 2 L of 1 N HCl was added. The mixture was allowed to stand at room temperature for one hour and then heated at ~105°C. When the linters were reduced to small pieces, the reaction mixture was stirred at 600 r.p.m. The heating was continued for an additional 1.5–2.0 h. The reaction mixture was then cooled to room temperature and filtered. The white powder obtained was washed with distilled water until pH between 5 and 7 and then dried at room temperature until passed freely through a US #20 mesh (850 μm) screen and contained moisture content (MC) of ~5%.

Preparation of CII-SiO_2 composites by spray drying

Appropriate amounts of MCCII slurry and SiO_2, equivalent to give 98:2, 95:5, 90:10, and 80:20 w/w ratios, were mixed and diluted with distilled water to obtain a 3% dispersion using a homogenizer (Biospec products, Inc., Bartlesville, OK) for 10 min at 10,000 r.p.m. A Yamato Pulvis spray-drier (Model GB-22, Yamato Scientific, Co. Tokyo, Japan) was employed at the previously optimized spraying conditions of inlet air temperature (IT) 195°C; atomizing air pressure (AA) 1.0 kg-f/cm^2; drying air rate (DA) 0.44 m^3/min; feed flow rate (FR) 2.0 ml/min and nozzle diameter (ND) 0.7 mm.

Preparation of CII-SiO_2 composites by wet granulation

Appropriate amounts of MCCII slurry and SiO_2, equivalent to give 98:2, 95:5, 90:10, and 80:20 w/w ratios, were mixed and diluted with distilled water to obtain a 5% dispersion using a homogenizer (Biospec products, Inc., Bartlesville, OK) for 10 min at 10,000 r.p.m. at room temperature. The resulting homogeneous mixture of CII:SiO_2 was collected by vacuum filtration and then sequentially granulated on an Erweka oscillating granulator (Model AR400, Chemical and Pharmaceutical Industry, Inc., New York, NY) using a 710 μm, 250 μm and 150 μm aperture screen size when the moisture content was ~45, 30 and 20%, respectively. The granules obtained were dried, either in air or in a convection oven at 35°C until the moisture content was less than 5%.

Preparation of CII-SiO_2 Composites by spheronization

An slurry of CII:SiO_2 at 98:2, 95:5, 90:10, and 80:20 w/w ratios were prepared as described under "*Preparation of CII-SiO_2 Composites by Wet granulation*". The resulting CII:SiO_2 mixture was collected by vacuum filtration and tray dried at room temperature until moisture content between 40 and 50% and then sequentially granulated in an Erweka oscillating granulator (Model AR400, Chemical and Pharmaceutical Industry, Inc., New York, NY) equipped with a 710 μm screen size. The extrudate was further dried to a moisture content of ~30% and then

extruded using the same granulator in a 250 μm screen size. The drying procedure was repeated until a moisture content of ~20% and extruded one more time in a 150 μm screen size. The extruded thus obtained was put in the spheronizer chamber (Marumerizer, Model QJ-230T, Fuji Paudal Co. Ltd., Charlotte, NC), which was operated at 1000 r.p.m. from 10 to 15 min to produce beads, which were then dried until moisture content lower than 5%.

Powder properties and characterization methods

Approximately 10 g of cellulose II:SiO_2 composites were fractionated for 30 min on a Ro-Tap sieve shaker (Model, RX29, W.S. Tyler Company, Mentor, OH) using stainless steel 600, 420, 250, 177,150, 125, 105, 75, 53, 45, and 38 μm size sieves, stacked together in the order mentioned. The fraction retained between 150 and 420 μm of spheronized products was used for the physical characterization since this fraction had particle size matches that of Celphere203. For cellulose II alone, the fraction that contained particles between 75 and 125 μm corresponding to an average particle size of about 90 μm was used in the study. The geometric mean diameter d_g, was determined from the log-normal distribution plot constructed between sieve mean diameter versus cumulative percent frequency using the Minitab software (version 15, Minitab, Inc., State College, PA).

Degree of crystallinity (DC) was obtained on a Siemens powder X-ray difractometer (Model D5000), equipped with monochromatic CuK ($\alpha1$ = 1.5460 Å, $\alpha2$ = 1.54438 Å). The Diffrac® Plus diffraction software (Eva, version 2.0, Siemens Energy and Automation, Inc., Madison, WI) was used for the data analysis. DC was calculated using the expression: % DC = 100* $I_C/(I_C + I_a)$, Where, I_C is the sum of the areas of all diffracted intensity of X-rays peaks and I_a is the area of the diffuse halo due to the amorphous region.

A helium displacement micropycnometer (Model MPY-2, Quantachrome Corporation, Boyton Beach, FL) was employed to obtain the materials true density. Samples were dried in a vaccum desiccator (Precision scientific Co., Chicago, IL) at 60°C and at a reduced pressure of 60 μm Hg for 24 h, followed by purging with helium for at least 40 min, before each measurement. The true density was calculated by dividing the mass of the material by its volume obtained from the equation: Vp = Vc– Vr(P_1/P_2 - 1), where, Vp is the volume of the powder, Vc is the cell volume, Vr is the reference cell volume, P_1 is the pressure in the cell, and P_2 is the pressure outside the cell.

Bulk density (ρ_{bulk}) was obtained directly from ratio of 20 g powder and its volume measured in 100 ml graduate cylinder. Tap density (ρ_{tap}) was determined using a VanKel tap density analyzer (Model 50–1000, VanKel Industries, Cary, NC) measuring the volume after 1200 taps. Porosity (ε) of the powder was determined from the equation: $\varepsilon = (1-\rho_{bulk}/\rho_{true})*100\%$.

Degree of polymerization was obtained by the intrinsic viscosity [η] method (ASTM D 1795; USP 28/NF23, 2005) at 25 ± 0.5°C using an Oswald capillary viscometer (size 50) and cupriethylenediamine hydroxide (CUEN) as the solvent, according to the relationship: DP = 190*[η].

Loss on drying was obtained using a mechanical convection oven (Model STM 80, Precision Scientific, Inc., Chicago, IL) at 105°C for 3 h. Flow rate was measured in a custom made flowmeter which consisted of a stainless steel cylinder (2.5 × 20.0 cm), equipped with a steel plates with a circular orifice (19.1 mm). Flowability was determined by filling the cylinder with ~20 g of the powder and measuring the time of flow through the orifice.

Morphology of the composite materials

SEM photographs were obtained using a scanning electron microscope (Model S-4800, Hitachi, Hitachi High Technologies America, Inc., and Pleasanton, CA). The powder was fixed on an aluminum stub using a double-sided adhesive tape and coated using a sputter coater (Model, Emitech K550). Samples were sputtered with a thin layer (3–5 nm) of gold/palladium (60:40) under an argon atmosphere for four minutes at 30 W. The acceleration voltage employed was 5 kV.

Energy dispersive X-rays spectroscopy (EDX)

A variable pressure scanning electron microscope (VP-SEM, Model 3400, Hitachi High Technologies America, Inc., Pleasanton, CA) was used to determine the distribution of SiO_2 on the materials. The X-rays were determined on a line scan mode using a Bruker AXS Microanalyzer (Model GmbH, Bruker AXS, Germany) at a live time of 90 sec, employing an acceleration voltage of 15 kV and 10 mm depth of field.

Water sorption analysis

It was performed on a VTI Symmetric Gravimetric Analyzer (Model SGA-100, VTI Corporation, Hialeah, FL), equipped with a chilled mirror dew point analyzer (Model Dewprime IF, Edgetech, Milford, MA). An initial drying phase at 60°C and a heating rate of 5°C/min, with continuous N_2 purging was executed. Runs were conducted at 25°C at relative humidity from 10 to 90%. Water uptake in the sample was considered at equilibrium when a weight change of no more than 0.01% was reached. Isotherms were fitted to the GAB (Guggenheim, Andersen and de-Boer) sorption model according to the equation[14]:

$$m = \frac{k*a*m_m*C}{(1-k-a)*(1-k*a+C*k*a)}$$

Where, m is the grams of water per gram of cellulose, m_m is the monolayer capacity (weight of water when the surface of one gram of cellulose is covered by a monolayer (g/g), "a" is the activity of water. C and k are energy constants for the monolayer and multilayer, respectively. The fitting procedure was performed using the Statgraphic software version 5 (StatPoint, Warrenton, VA).

Surface area analysis

It was performed using a Quantasorb sorption system (Quantachrome Corp., Boyton Beach, FL). Helium gas

was used as carrier diluents gas; while nitrogen gas was used as adsorbate. A capillary cell (part # 74002) was used for the analysis. Before performing the surface area measurements, samples were dried in a vacuum oven (Model 68351, Precision scientific Co., Chicago, IL) at 60°C and at 40 mm Hg for 24 h. Measurements were conducted at relative pressures (P/P_0) ranging from 0.05 to 0.25 and the specific surface area was obtained by the BET method[15].

Contact angle analysis

Compacts (diameter, 13 mm), each weighing 500 mg, were made at a 0.9 solid fraction. The contact angle measurements were determined on a contact angle goniometer (Model A100-00, Rame-Hart, Inc., Mountain Lakes, NJ) according to the sessile drop method. An image analysis camera (Model 100-22, Rame-hart, Inc., Mountain Lakes, NJ) was used for the data analysis. A droplet of ~25 µL of water was put carefully onto the upper surface of the tablet and the contact angle was reported after 6 s of spreading.

Swelling studies

Swelling was expressed as the ratio of the expanded volume of the powder after uptaking water and the initial sample weight. The method of Edge and collaborators was used[16,17]. Briefly, ~500 mg of the powder was vigorously dispersed in a graduate cylinder filled with 10 ml of distilled water at room temperature. The cylinder was placed on a flat surface and the increase in volume was measured after 5 days.

Tableting properties

Approximately, 500 mg of powder was compressed on a single tablet press (Model C, Carver Press, Menomonee Falls, WI) at pressures ranging from 10 to 260 MPa using a flat-faced 13 mm punch and die set at a dwell time of 30 s. The upper punch was equipped with a load cell (Model: LCGD-10K, Range 0-10000 lbs, Omega Engineering, Inc., Stamford, CT) and a strain gauge meter (Model: DP25B-S, Omega Engineering, Inc., Stamford, CT). Tablets were kept in a desiccator over Drierite® for 48 h before the analysis.

The radial tensile strength (TS) values were obtained according to the Fell and Newton equation from the breaking force given by the load-deflection curves[18].

$$TS = \left[\frac{2F}{\pi * D * t}\right]$$

Where, F is the breaking force needed to break the compact into two halves, D is the diameter of the compact (mm), and t is the compact thickness (mm). The data of radial tensile strength versus the product of the solid fraction and the compression pressure was fitted according to the Leuenberger model[19].

$$TS = T_{max} * (1 - e^{(-\gamma c * P * \rho_r)})$$

Where, TS is the radial tensile strength (Mpa), T_{max} is the theoretical tensile strength at infinite compression pressure, γ_c is the compression susceptibility parameter (Mpa^{-1}), ρ_r is the compact relative density and P is the compression pressure. Data fitting was performed employing the Statgraphic® software (StatPoint Technologies, Warrenton, VA).

Tablet disintegration tests were performed in distilled water according to the USP 34/NF29 specifications, employing an Erweka GmbH disintegration apparatus (type 712, Erweka, Offenbach, Germany).

Results and discussion

Powder XRD

The powder XRD of (MCCII), SiO_2, SD-CII:SiO_2 composites, and cellulose I materials is shown in Figure 1. CII and CII:SiO_2 composites showed peaks at 12, 20 and 22° 2θ due to the 1 ī 0, 110 and 200 reflections, respectively, confirming the presence of the cellulose II lattice. Prosolv® SMCC90, Prosolv® SMCC50 and Celphere203, in contrast, displayed characteristic diffraction peaks due to the cellulose I lattice at 14.8, 16.3 and 22.4° 2θ, corresponding to the 1 ī 0, 110 and 200 reflections, respectively[20]. A shoulder at 20.4° 2θ has also been also identified in some cellulose I excipients[21]. On the contrary, SiO_2 showed a diffused halo indicating its amorphous nature. The 2% SiO_2 content in Prosolv® materials did not modified the cellulose I XRD patterns since Celphere203 does not possess SiO_2 and showed the same crystalline peaks than Prosolv® materials. Tobyn and coworkers previously reported that silicification does not change the crystalline peaks of cellulose I[22]. As seen in Table 1, the degree of crystallinity (DC) of all spray dried composites was slightly lower compared to that of MCCII (~68%). Since SiO_2 is completely amorphous, its presence in the wet granulated and spheronized products led to a decrease in the intensity of diffraction peaks, especially at a silicification level of 20%. The DC of commercial cellulose I excipients has been reported to range between 65 and 80% and Celphere203 presented the lowest DC[23].

Particle size distribution

Figure 2 shows the particle size distributions of CII:SiO_2 composites. Most materials presented a positively skewed distribution. Spray dried products presented the narrowest distribution of particle size followed by the wet granulated and spheronized products. The distributions of particle size of commercial materials such as Prosolv® SMCC50, Prosolv® SMCC90 and Celphere203 are close to those materials obtained by spray drying, wet granulation and spheronization, respectively. Spray dried materials showed geometric mean diameters from 51 to 71 µm. This includes the value of Prosolv® SMCC50 (58 µm). It has been previously demonstrated that small particle sizes are usually obtained when small scale spray driers are employed[24]. Wet granulated products exhibited geometric mean diameters from 105 to 130 µm. The corresponding value for Prosolv® SMCC90 was 110 µm. Spheronized

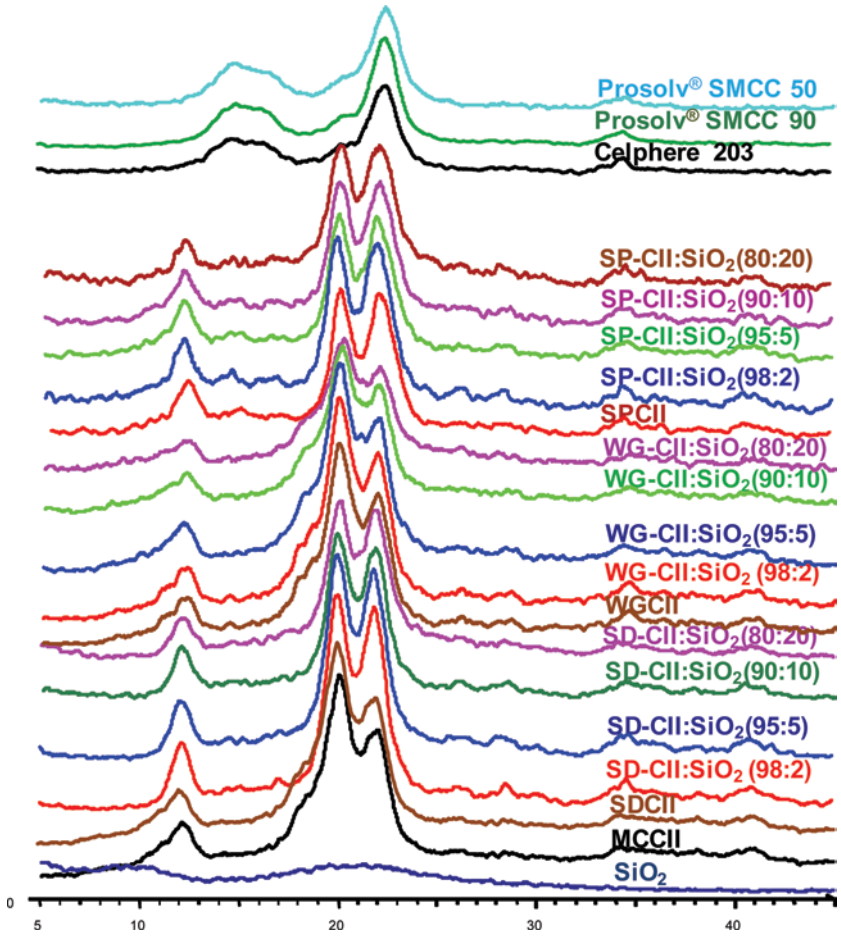

Figure 1. Powder XRD of CII:SiO_2 composites and commercial cellulose I materials.

Table 1. Powder properties of the SD-CII-SiO_2 composites and Prosolv SMCC50.

Material	True density (g/cc) $n=3$	Loss on drying (%) $n=1$	Bulk density (g/cc) $n=3$	Tap density (g/cc) $n=3$	Hausner ratio $n=3$	Powder porosity $n=3$
MCCII	1.54 ± 0.02	3.1	0.38 ± 0.03	0.54 ± 0.06	1.44 ± 0.05	0.76
SD-CII	1.55 ± 0.01	2.8	0.55 ± 0.00	0.81 ± 0.01	1.46 ± 0.03	0.64
SD-CII:SiO_2(98:2)	1.55 ± 0.01	2.7	0.48 ± 0.01	0.73 ± 0.05	1.52 ± 0.08	0.69
SD-CII:SiO_2(95:5)	1.57 ± 0.00	3.1	0.45 ± 0.00	0.69 ± 0.03	1.53 ± 0.07	0.70
SD-CII:SiO_2(90:10)	1.60 ± 0.00	2.4	0.42 ± 0.01	0.66 ± 0.04	1.57 ± 0.13	0.73
SD-CII: SiO_2(80:20)	1.67 ± 0.00	2.8	0.36 ± 0.00	0.65 ± 0.02	1.79 ± 0.06	0.78
Prosolv® SMCC50	1.56 ± 0.01	3.0	0.32 ± 0.00	0.44 ± 0.01	1.35 ± 0.02	0.79

Material	Degree polymerization $n=5$	Specific surface area (m^2/g) $n=3$	Degree of crystallinity (%) $n=3$	Geometric mean diameter (μm) $n=1$	Flow rate (g/s) (19.1 mm) $n=3$
MCCII	78.6 ± 5.1	0.5 ± 0.1	68.0 ± 1.4	258 ± 42	3.3 ± 0.1
SD-CII	79.1 ± 5.5	1.6 ± 0.0	62.6 ± 2.3	66 ± 6	4.0 ± 0.3
SD-CII:SiO_2(98:2)	85.5 ± 7.4	3.9 ± 0.1	62.4 ± 1.3	61 ± 9	6.9 ± 0.7
SD-CII:SiO_2(95:5)	95.1 ± 4.9	10.5 ± 0.1	62.3 ± 3.8	64 ± 9	6.7 ± 1.0
SD-CII:SiO_2(90:10)	94.2 ± 8.2	20.9 ± 0.4	63.3 ± 1.0	75 ± 9	4.7 ± 4.7
SD- CII: SiO_2(80:20)	85.1 ± 1.3	41.4 ± 1.4	56.8 ± 0.6	51 ± 5	2.2 ± 0.7
Prosolv® SMCC50	191.7 ± 6.1	6.3 ± 0.0	67.6 ± 1.8	58 ± 5	5.5 ± 0.6

materials presented geometric means from 148 to 558 μm and included that of Celphere203 (303 μm). This technique usually renders beads of about 1000 μm, but in this case by using the same screens from the wet granulated materials for the extrudate, the size of the resulting beads was greatly reduced. Thus, by controlling the screen size in the granulation process, the size of the granules and beads was successfully reduced.

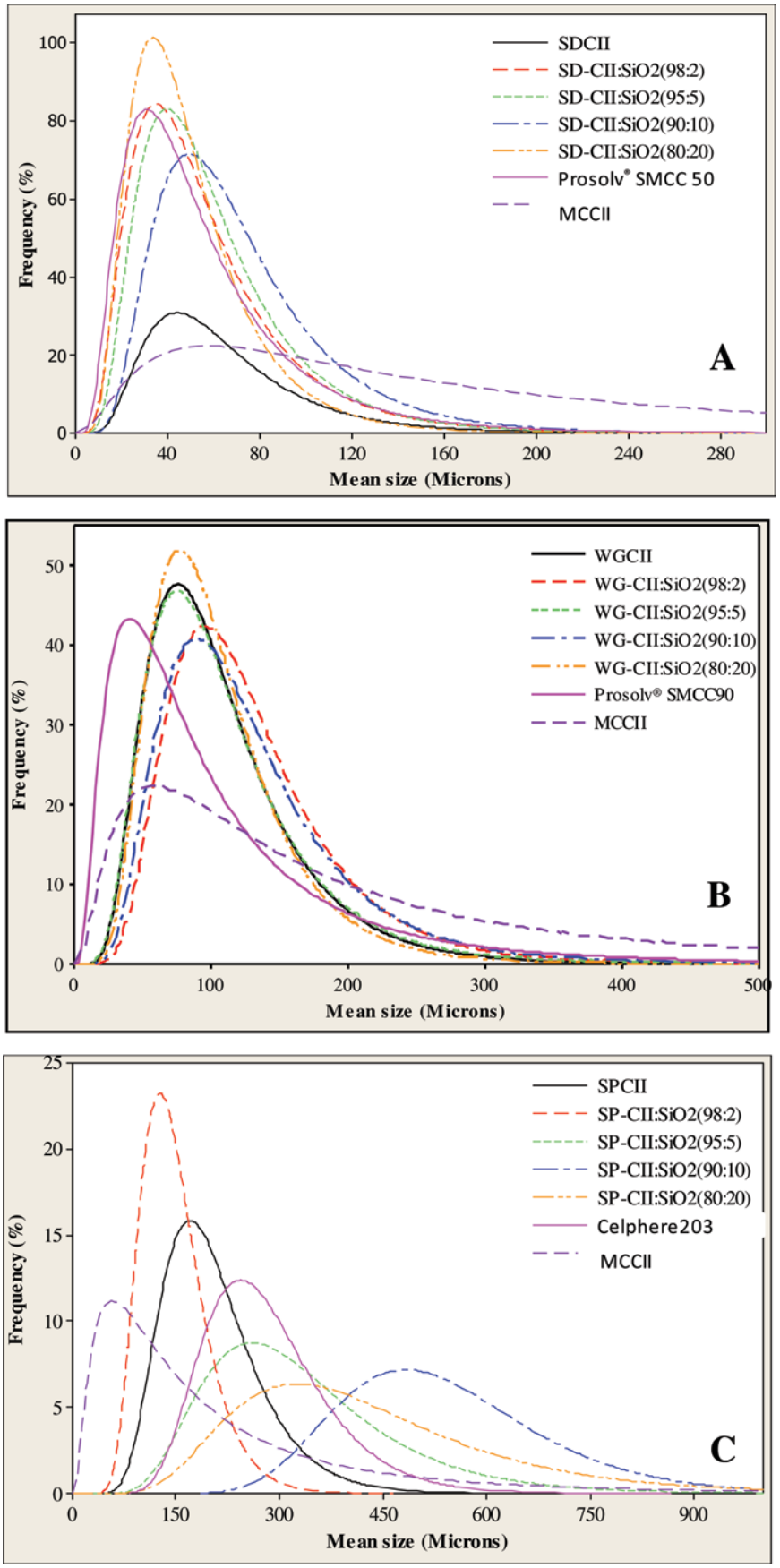

Figure 2. Particle size Distribution of (A) spray-dried, (B) wet granulated, (C) spheronized CII:SiO_2 composites.

Morphological characterization

Figure 3 shows the chain aggregate conformation of commercial materials. SiO_2 is formed by semispherical particles of sizes from 30 to 50 nm. On the contrary, MCCII has a fibrous nature as obtained from cotton linters without further processing. Prosolv® SMCC50 and Prosolv® SMCC90 are spray dried cellulose I:SiO_2(98:2) materials which are formed by aggregates of irregular shape. Tiny chunks of SiO_2 are homogeneously distributed on the surface of cellulose I and possibly in the core of Prosolv®s making its surface rougher and highly porous. Celphere203 presented a smooth and non-porous surface and spherical shape. It is also a cellulosic I material, but produced by spheronization. Figure 4 shows that the original fibrous shape of MCCII was modified by the spray drying, wet granulation and spheronization processes. It is expected that modification in morphology also causes changes in the powder properties. Surface roughness of the spray dried composites increases as the amount of SiO_2 increases. For the case of highly silicified samples presenting SiO_2 content higher than 10%, the surface of the particles is highly rough and cracked forming isolated SiO_2 chunks or clusters superimposed on top of each other, possibly, leading to a non-uniform and overlapped coverage of SiO_2 on the surface of cellulose. Wet granulation produced granules of irregular shape and highly rough surfaces. During wet granulation the wet fibers coalesced and formed larger particles which are shaped or molded when they passed through the orifice of the screens. As the level of SiO_2 increased

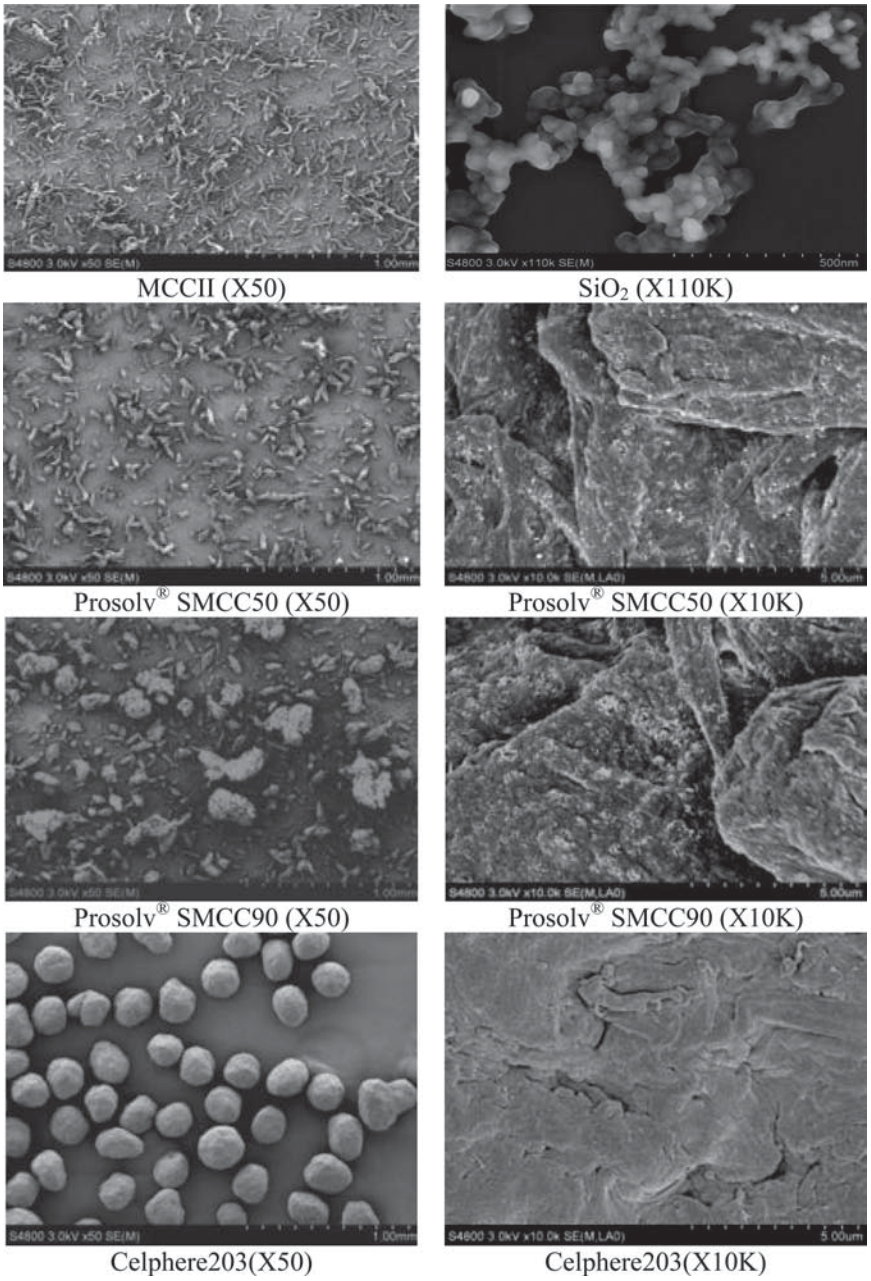

Figure 3. SEM Microphotographs of MCCII, SiO_2 and commercial cellulose I materials.

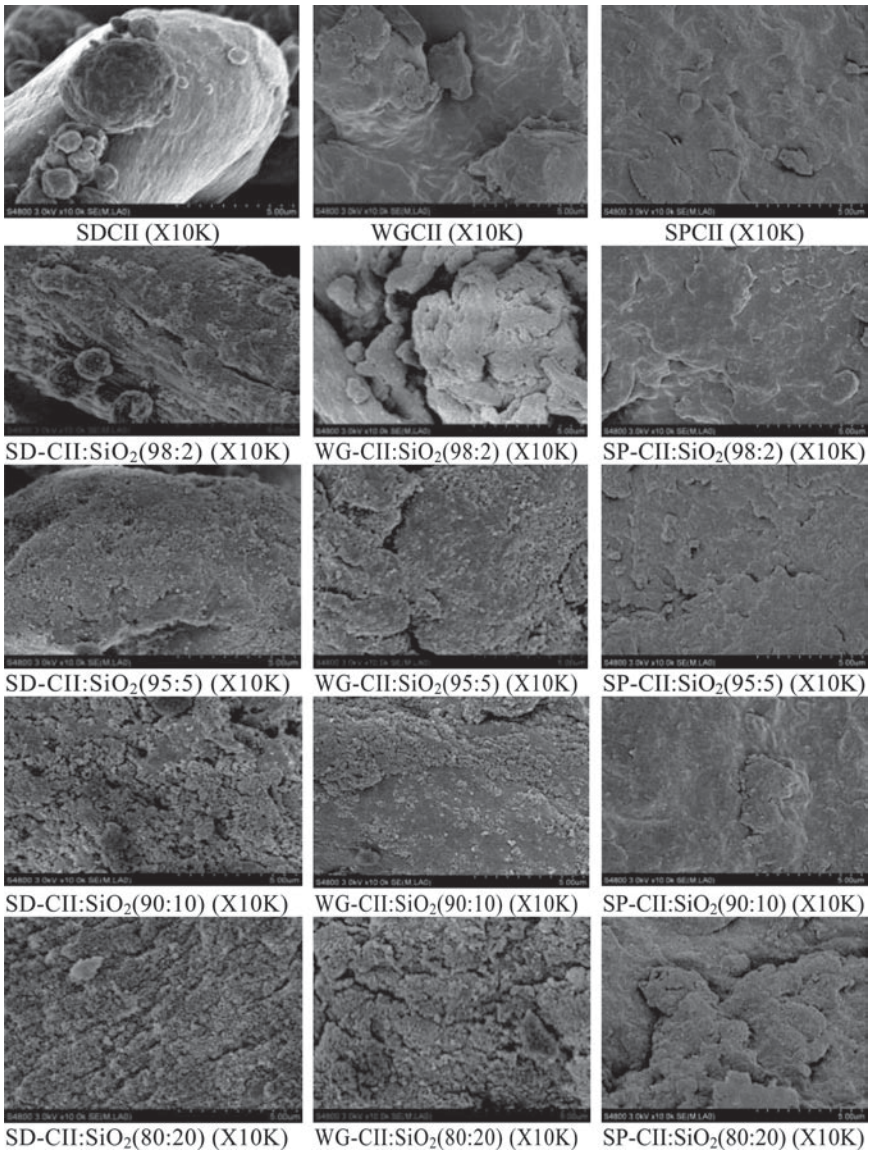

Figure 4. SEM Microphotographs of the CII:SiO_2 composites.

more roughly features are visible due to deposition of chunks or clusters of SiO_2 on the surface and probably on the core of the granules, especially at the SiO_2 level of 20%. Granules extruded in the granulator were molded in the spheronizer which cut off and round off all the sharp and roughly surfaces making the surface of the particles smoother, less porous and shape nearly spherical. Silicification levels up to 10% did not cause any change on the surface of the composite materials. Only the SiO_2 level of 20% rendered a product with a rough surface due to a large amount of SiO_2 present. The morphology and surface appearance of SPCII was very similar to the one observed for Celphere203 indicating that only particle shape, but not surface characteristics were silicification independent.

Distribution of SiO_2

Figure 5 shows the EDS images for the spray dried, wet granulated and spheronized materials. The intensity of the SiO_2 signal increased as the amount of SiO_2 increased. SiO_2 covered completely the surface of cellulose at all levels of silicification for the spray-dried materials. It is also possible that some individual SiO_2 aggregates be formed at silicification levels higher than 10%. Coverage of SiO_2 in the wet granulated materials increased as the amount of SiO_2 increased. SiO_2 was also absent in the holes, cracks and cavities of the samples, indicating a non-homogeneous coverage. Perhaps during the granulation process SiO_2 moves around the wet mass forming SiO_2 patches. It is also plausible that part of SiO_2 is entrapped inside the core of the granules. The 20% level of silicification seems to achieve a complete coverage of the surface of the granules. Spheronized materials showed a smooth SiO_2 distribution at all levels. Chunks of SiO_2 are less evident in these samples. No protrusions or features were visible on the surface. The cross-sectional area of the beads evidenced that at all levels SiO_2 was also present in the core. Silicification levels from 2 to

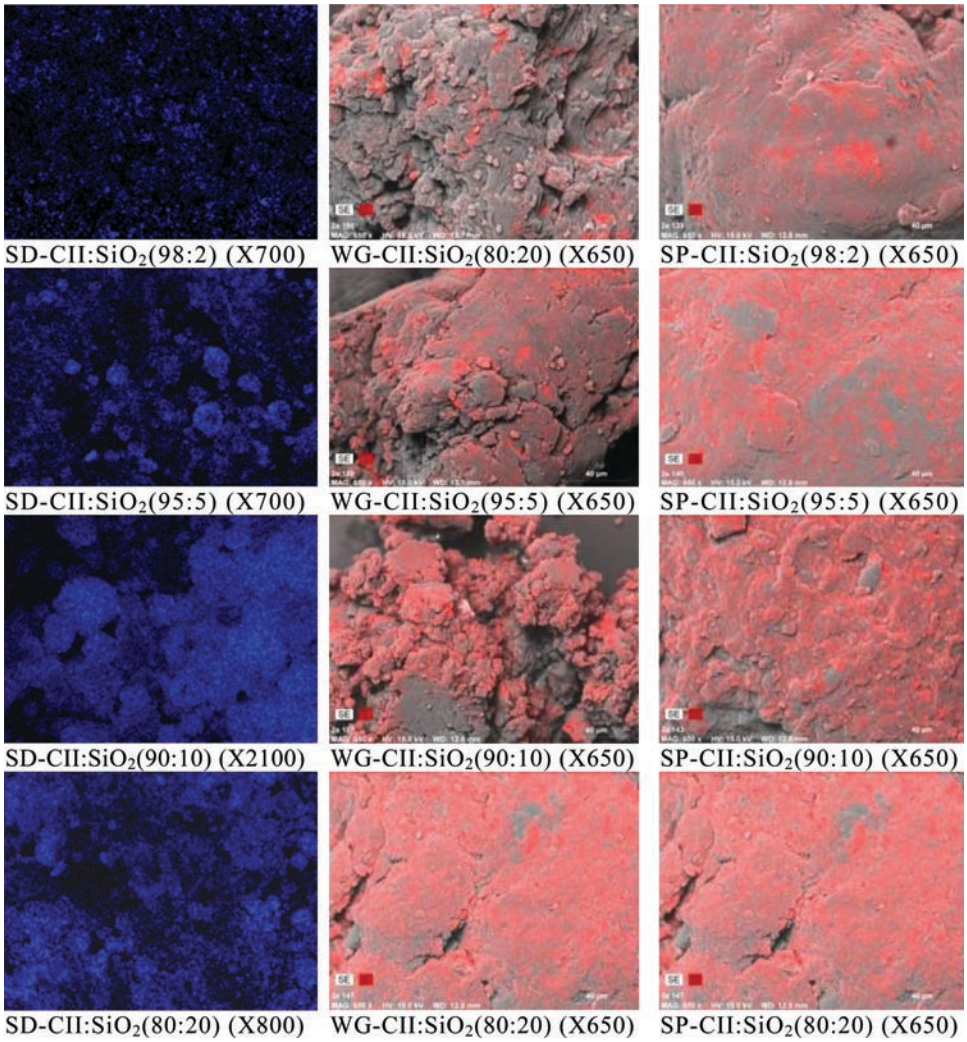

Figure 5. Distribution of SiO_2 on the surface of CII:SiO_2 composites.

5% rendered beads with a complete distribution of SiO_2 inside the core and the formation of few isolated chunks. Results indicate that in spheronized materials most of the SiO_2 was present inside the beads rather than on the surface. Prosolv samples with a 2% silicification exhibited a homogeneous coverage of the surface. No chunks or aggregates of SiO_2 are observed. The holes and cavities of Prosolv® SMCC50 seem to be covered more evenly than for Prosolv® SMCC90 because Prosolv® SMCC50 particles are smaller and thus, SiO_2 particles are able to penetrate cavities more deeply.

Powder Properties

Powder properties of the CII:SiO_2 composites are summarized in Tables 1, 2 and 3 for the spray dried, wet granulated and spheronized products, respectively. True density of the composites increased at >10% silicification levels. This trend was observed in all silicified materials independent of the process employed. In fact, the values of true density independent of the process employed were about of the same magnitude for each silicification level. SiO_2 itself possesses a higher true density (2.27 g/cc) than MCCII (~1.54 g/cc). Thus, the resulting physical mixture of both materials at >10% SiO_2 levels increased true density of the composites compared to CII. The moisture content for all materials was <4.0 % w/w indicating that silicification did not contribute to moisture of CII because SiO_2 *per se* has a very low moisture content (~1.5%).

Compared to CII alone, silicification levels up to 10% caused an increase in the bulk and tap densities of samples when spray drying and wet granulation are employed. Silicification in the spheronized process has no effect on the bulk and tap density of CII. In this case, the high contribution of silicification was made by the spheronization process, rather than silicification. The spherical geometry and the large particle size played a major role on the bulk and tap density restricting the effect of silicification. Celphere203 had high bulk and tap densities suggesting that these two variables depended on the particle shape and size given by spheronization. Since CII, SD/WG:SiO_2(80:20), Prosolv® SMCC50 and Prosolv® SMCC90 have very low bulk and tap densities, they can be used in the production of high dose tablets in which bulky compacts are not desirable. The low bulk and tap densities observed for SD/WG-CII-SiO_2 (80:20) could be

Table 2. Powder Properties of the WG-CII-SiO_2 composites and Prosolv90.

Material	True density (g/cc) $n=3$	Loss on drying (%) $n=1$	Bulk density (g/cc) $n=3$	Tap density (g/cc) $n=3$	Hausner ratio $n=3$	Powder Porosity $n=3$
MCCII	1.54 ± 0.02	3.1	0.38 ± 0.03	0.54 ± 0.06	1.44 ± 0.05	0.76
WG-CII	1.56 ± 0.00	3.6	0.64 ± 0.01	0.79 ± 0.00	1.23 ± 0.00	0.59
WG-CII:SiO_2(98:2)	1.55 ± 0.01	3.0	0.61 ± 0.00	0.77 ± 0.00	1.27 ± 0.00	0.61
WG-CII:SiO_2(95:5)	1.57 ± 0.01	2.9	0.58 ± 0.00	0.72 ± 0.02	1.23 ± 0.00	0.63
WG-CII:SiO_2(90:10)	1.60 ± 0.00	3.0	0.55 ± 0.01	0.68 ± 0.02	1.24 ± 0.10	0.66
WG- CII: SiO_2(80:20)	1.66 ± 0.00	2.4	0.28 ± 0.00	0.36 ± 0.00	1.29 ± 0.00	0.83
Prosolv® SMCC 90	1.55 ± 0.00	3.3	0.28 ± 0.00	0.36 ± 0.00	1.29 ± 0.00	0.82
Material	Degree polymerization $n=5$	Specific surface area (m^2/g) $n=3$	Degree of crystallinity (%) $n=3$	Geometric mean diameter (μm) $n=1$	Flow rate (g/s) (19.1 mm) $n=3$	
MCCII	78.6 ± 5.1	0.5 ± 0.1	68.0 ± 1.4	258 ± 42	3.3 ± 0.1	
WG-CII	97.2 ± 1.4	0.4 ± 0.0	67.5 ± 1.3	107 ± 6	19.3 ± 0.1	
WG-CII:SiO_2(98:2)	87.4 ± 4.7	1.1 ± 0.1	63.1 ± 2.4	129 ± 7	19.9 ± 0.1	
WG-CII:SiO_2(95:5)	87.8 ± 2.6	6.6 ± 0.1	57.1 ± 1.1	110 ± 7	18.5 ± 0.0	
WG-CII:SiO_2(90:10)	88.6 ± 6.6	16.2 ± 0.1	56.5 ± 2.9	128 ± 6	15.7 ± 1.1	
WG- CII: SiO_2(80:20)	76.9 ± 5.6	28.3 ± 1.3	53.6 ± 1.1	105 ± 6	15.9 ± 0.6	
Prosolv® SMCC90	2.4 ± 4.2	5.5 ± 0.0	67.1 ± 1.8	110 ± 9	8.2 ± 0.1	

Table 3. Powder properties of the SP-CII-SiO_2 composites and Celphere203.

Material	True density (g/cc) $n=3$	Loss on drying (%) $n=1$	Bulk density (g/cc) $n=3$	Tap density (g/cc) $n=3$	Hausner ratio $n=3$	Powder Porosity $n=3$
MCCII	1.54 ± 0.02	3.1 ± 0.3	0.38 ± 0.03	0.54 ± 0.06	1.4 ± 0.1	0.76
SPCII	1.55 ± 0.01	2.1 ± 0.1	0.78 ± 0.01	0.90 ± 0.01	1.2 ± 0.0	0.50
SP-CII:SiO_2(98:2)	1.56 ± 0.01	2.6 ± 0.1	0.77 ± 0.00	0.91 ± 0.04	1.2 ± 0.1	0.50
SP-CII:SiO_2(95:5)	1.57 ± 0.00	1.4 ± 0.1	0.78 ± 0.02	0.88 ± 0.02	1.1 ± 0.0	0.51
SP-CII:SiO_2(90:10)	1.60 ± 0.00	2.2 ± 0.1	0.78 ± 0.01	0.89 ± 0.02	1.1 ± 0.0	0.51
SP- CII: SiO_2(80:20)	1.67 ± 0.01	2.3 ± 0.5	0.78 ± 0.01	0.87 ± 0.01	1.1 ± 0.0	0.53
Celphere203	1.50 ± 0.01	5.3 ± 0.0	0.86 ± 0.01	0.99 ± 0.03	1.1 ± 0.0	0.43
Material	Degree polymerization $n=5$	SSA (m^2/g) $n=3$	Degree of crystallinity (%) $n=3$	Geometric mean diameter (μm) $n=1$	Flow rate (g/s) (19.1 mm) $n=3$	
MCCII	78.6 ± 5.1	0.5 ± 0.1	68.0 ± 1.4	258 ± 42	3.3 ± 0.1	
SPCII	74.4 ± 5.4	0.3 ± 0.0	68.0 ± 1.4	207 ± 39	31.7 ± 0.9	
SP-CII:SiO_2(98:2)	80.2 ± 3.5	0.3 ± 0.0	64.6 ± 0.7	148 ± 4	32.4 ± 1.7	
SP-CII:SiO_2(95:5)	71.7 ± 3.2	0.4 ± 0.0	61.1 ± 0.4	339 ± 18	40.5 ± 0.2	
SP-CII:SiO_2(90:10)	79.7 ± 2.6	1.3 ± 0.1	56.1 ± 1.6	558 ± 21	39.8 ± 0.4	
SP- CII: SiO_2(80:20)	70.8 ± 3.0	1.7 ± 0.0	52.9 ± 2.5	450 ± 33	22.7 ± 2.3	
Celphere203	230.3 ± 5.3	0.2 ± 0.0	52.1 ± 1.2	303 ± 7	41.0 ± 0.2	

attributed to the high contribution of the light and bulky SiO_2 which has a reported $\rho_{bulk}=0.03$ and $\rho_{tap}=0.05$ g/cc, respectively[25].

The degree of cohesiveness given by the Hausner ratio increased as the level of silicification increased in the spray dried products. On the contrary, this trend was not observed for the wet granulated and spheronized materials. Overall, materials produced by spray drying were more cohesive than the ones produced by wet granulation and spheronization. Since spray dried products and MCCII had Hausner ratio values larger than 1.4, they are considered cohesive with high interparticular friction. Cohesiveness of the commercial products ranged as Prosolv SMCC50>Prosolv SMCC90>Celphere203. This suggests that cohesiveness depended on particle size and density. Likewise, cohesiveness followed the trend spheronized<wet granulated<spray-dried indicating that as particle size and density increases, cohesiveness decreases.

The processes employed decreased porosity of MCCII. This means that the fibrous shape is transformed into one that is able to pack more decreasing voids spaces in the powder. Compared to SDCII and WGCII which were processed without the addition of SiO_2, the total powder porosity of the composites increased as the amount of SiO_2 increased due to a more coating effect of SiO_2 on the surface of the particles. On the contrary, silicification had no effect of the porosity of the beads. In this

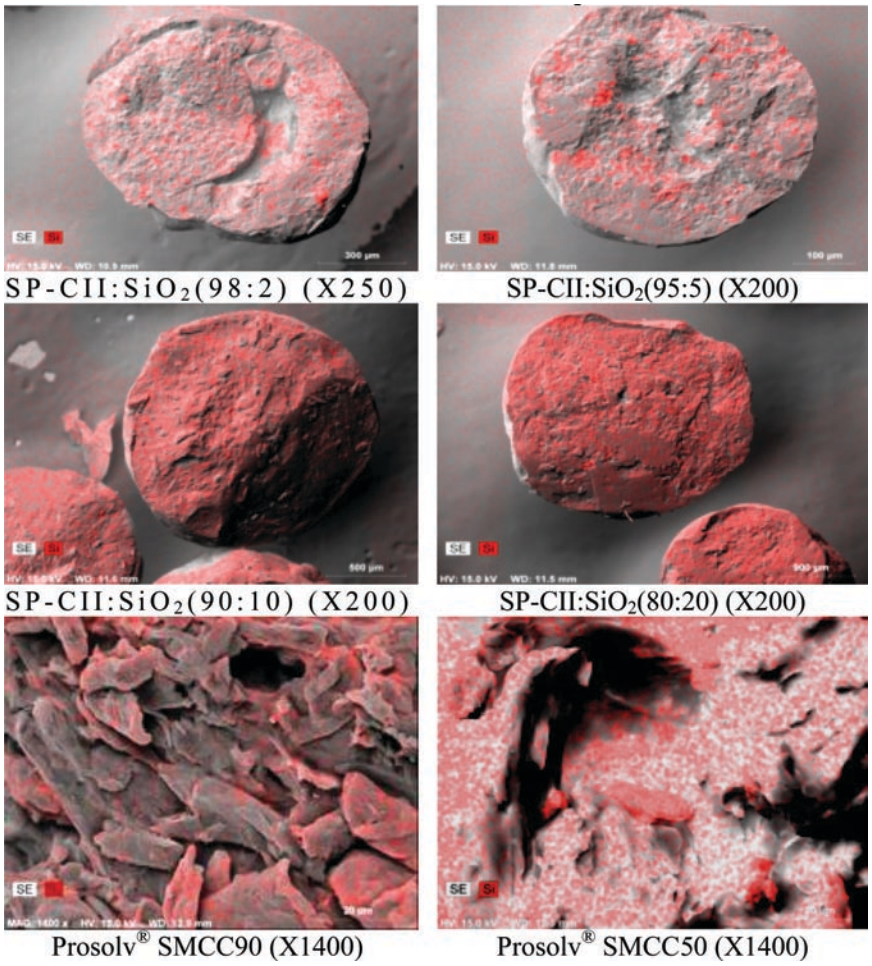

Figure 6. Distribution of SiO_2 in the core of the spheronized CII-SiO_2 composites and on the surface of commercial cellulose I products.

case, the spheronized process produced smooth beads preventing or correcting any rough defect due to silicification. Prosolv® SMCC50, Prosolv® SMCC90 had high powder porosities (0.79 and 0.82, respectively), while Celphere203 due to its smooth surface had a very low porosity (0.43).

Neither silicification, nor process of manufacture produced a major change in the degree of polymerization of CII. This indicates that the viscosity of the CUEN-CII complex was not affected by the presence of SiO_2. Nonetheless, Prosolv SMCC50 and Prosolv SMCC90 and Celphere203 exhibited a higher degree of polymerization (DP) than coprocessed materials. It has been reported that cellulose I has higher DP and molecular weight than MCCII[26].

Silicification increased the specific surface area (SSA) of CII. Spray drying was the most effective process to disperse SiO_2 on the surface of the particles since it rendered the largest values of SSA. On the contrary, the spheronization process rendered the lowest SSA values probably due to the fact that part of the SiO_2 was also incorporated in the core which is more inaccessible and as a result, beads had low porosities and smooth surface, preventing nitrogen molecules from accessing the core of the beads. Wet granulated materials presented SSA values in between.

The way in which gravity overcomes the cohesive forces and the interlocking structure of the materials is reflected in their flow. Silicification at 2% and 5% levels produced a material with the best flow. In fact, these values were ~2-fold higher than the one obtained for MCCII, whereas, SD-CII:SiO_2(80:20) presented the lowest flow rates mainly due to high porosity, low bulk and tap densities; while, the low flow of MCCII was caused by its fibrous shape and hence particle interlocking, high porosity and low bulk and tap densities. The rough surfaces and indentations of Prosolv® SMCC50 and its natural aggregate structure might contribute to poor flow. Flow rates of the wet granulated materials are shown in Table 2. Their flow was ~6 times larger than the one produced by MCCII and ~25 larger than that of Prosolv® SMCC90. Prosolv® SMCC90 presented low flow values compared to the granules produced with or without silicification. The wet granulation process produced larger granules which had also larger bulk and tap densities than spray dried materials. SiO_2 levels higher than 10% in spray dried and wet granulated materials causes clusters on the surface of cellulose which might fall off from the particles causing friction and mechanical interlocking preventing flow. All spheronized materials had the highest flow rates (Table 3). Their values were comparable to

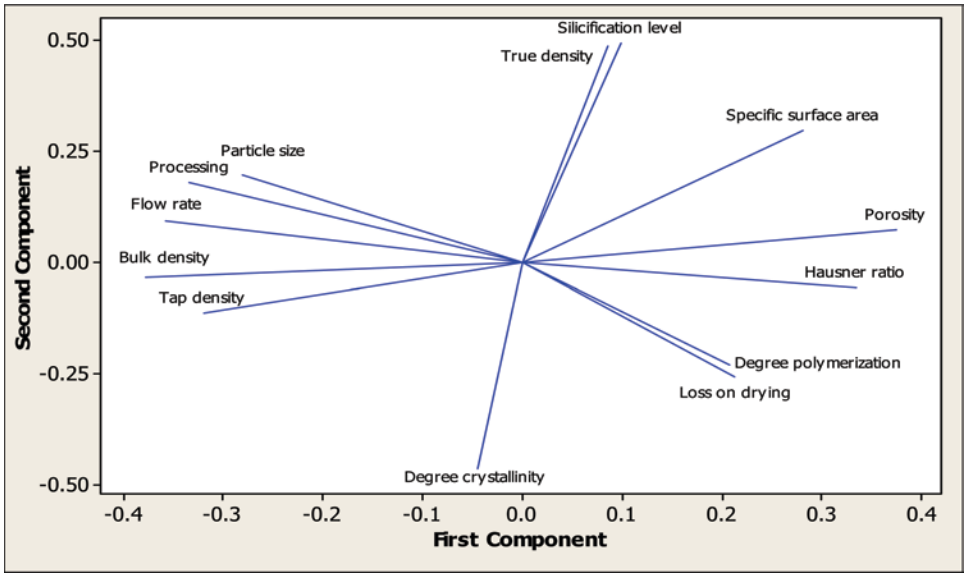

Figure 7. Loading plot of measured properties of MCCII and CII:SiO_2 composites.

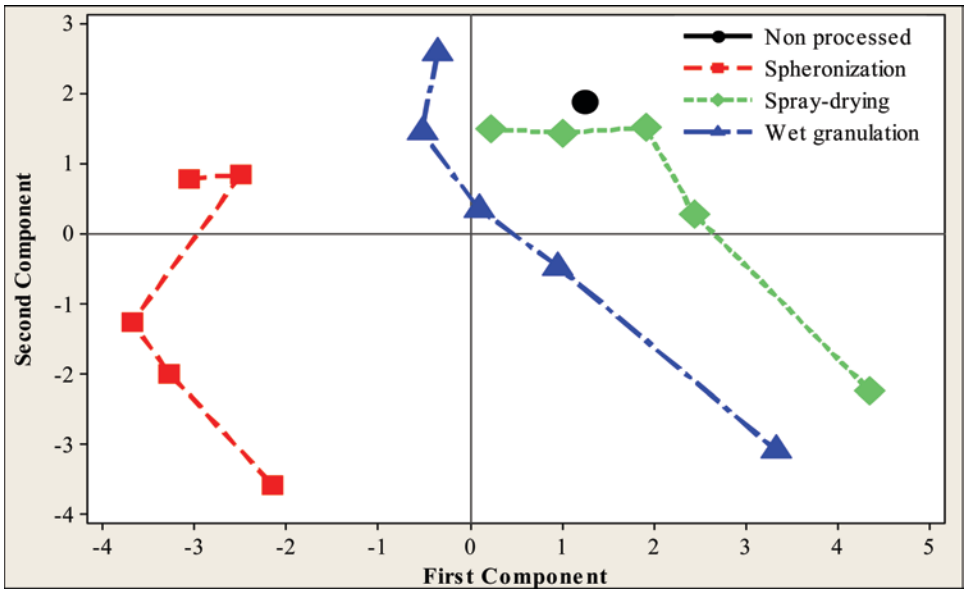

Figure 8. PCA score plot of measured properties for MCCII and CII-SiO_2 composites.

the one shown by Celphere203 and from 10 to 15 times larger than the one presented by MCCII. These results are not surprising since these materials had smooth surface, larger size, higher bulk and tap densities and low porosity. Compared to the parent MCCII, it is clear that both, silicification and process employed improved flow. The general trend for changes in flow due to processing was spheronization>wet granulation>spray-drying.

Principal component analysis (PCA)

PCA was conducted to determine the general trends of the powder properties altogether. The loading plot of measured properties is shown in Figure 7. The lines show the projections of the original powder properties on the principal component 1 and 2 (PC1 and PC2) using the coordinate scales on the X and Y axis, respectively. The numbers on the axis are in arbitrary units. The manufacturing process had a strong influence on properties such as particle size, flow rate, and bulk and tap densities. Similarly, porosity and bulk and tap densities were inversely correlated. Thus, powders with high porosity exhibited a very low density. Flow rates were inversely correlated to Hausner ratio. Silicification was correlated with true density and in a lower degree with the specific surface area of the materials. Likewise, silicification had a negative influence on degree of crystallinity of the materials.

Figure 8 shows the PCA score plot of the materials. The first component separates the spheronized materials from the spray dried and wet granulated ones. PC2 shows a decreasing trend with increasing silicification levels since it increased from top to bottom in the graph. Most

of the powder properties of MCCII and SD-CII and silicified materials up to 5% silicification were similar indicating no effect due to silicification. Likewise, SPCII and SPCII:SiO_2(98:2) showed similar properties too. Since the lines are straight in the last three points of each curve, the degree of change in magnitude of the powder properties is proportional at silicification levels higher than 5%, being the highest for the spray dried materials. Interestingly, processing or silicification levels up to 2% would not cause major changes in the powder properties.

Water properties

Figure 9 shows the GAB isotherms for water sorption and Table 4 shows the parameters derived from this model. Since CII is highly hydrophilic, the monolayer sorption capacity (m_m) indicates that only at the 20% level of silicification the affinity of MCCII for water is decreased. Thus, at this level a partial surface area is covered by water molecules because some of the binding sites of cellulose are already interacting via hydrogen bonding with SiO_2. Since MCCII is highly hydrophilic, it requires up to a 20% SiO_2 to have the same monolayer capacity than Prosolv® SMCC50 and Prosolv® SMCC90 which only contains a 2% of SiO_2. Both materials are cellulose I and are obtained from softwood and produced by spray drying. Celphere203 which is a cellulose I material presented the highest m_m (0.15) indicating a high affinity for water. On the contrary, SiO_2 presented the lowest m_m (0.02), indicating a low affinity for water compared to Celphere203 and cellulosic composites. This might be explained by its limited hydrogen bonding capacity compared to that of cellulosic products because SiO_2 has a limited formation of hydrogen bonds through its few sylanol groups and water. On the contrary, Celphere203 has a high ability to form hydrogen bonds through their hydroxyl groups and water. The energetic of monolayer adsorption (c) was higher than the energetic of multilayer (k). The energetic of monolayer varied as SiO_2 (100)> CII:SiO_2 composites>Celphere203 (1.0) and k values varied as SiO_2(1.0)> CII:SiO_2 materials>Celphere203 (0.6). Since k values for most materials were between 0.8 and 0.9, it is expected no distinction between multilayer molecules and liquid water, and thus, the multilayer molecules are not completely structured in layers but have some characteristics as the liquid. Further, since c values were the highest for SiO_2 and the lowest for Celphere203, water molecules are expected to be strongly bound to the substrate in SiO_2 and less firmly to Celphere203. In this material water molecules in the multilayer are strongly structured and differ considerably from the bulk liquid water due to the low k value (0.6).

Wetting results from intermolecular interactions when water and a solid surface are brought together. In all cases a complete wetting was achieved since water drops spread on top of the compacts with time with its initially nonzero contact angle moving towards its limiting equilibrium, zero value. Table 4 shows the contact angles after six seconds of spreading. In general, cellulose II materials exhibited more wettability than the cellulose I counterpart since after six seconds contact angles of Prosolv® SMCC50 and Prosolv® SMCC90 were ~24°, whereas those for the CII:SiO_2 composites were zero. On the contrary, compacts made of the spheronized CII:SiO_2 composites showed as much wettability as Celphere203 since within six sec contact angles move from ~45 to zero degrees. This result is consistent with its high hydrophilicity.

The swelling values of the spray dried, wet granulated and spheronized materials are shown in Table 4. Results indicate that silicification decreased the swelling values of SDCII and WGCII. A 20% silicification rendered a swelling value of ~0.25 ml/g, and 0.45 ml/g for spray dried and wet granulated products, which are comparable to Prosolv® SMCC50 and Prosolv® SMCC90. Opposed to spray dried and wet granulated materials, silicification levels had no contribution on the swelling values of SPCII. In this case, swelling behavior was more process-dependent, rather than silicification dependent. Probably, the smooth surface and low porosity produced by this process prevented water from penetrating the core of the particles and cause swelling. Celphere203 swelled as much as spheronized materials since the later were highly hygroscopic.

Tableting properties

The effect of silicification on the tensile strength of the spray dried materials is shown in Figure 10. Compared to MCCII, all composite materials showed higher tensile strengths. The compact tensile strength increased with the increasing applied pressure. The higher values obtained for the spray-dried materials are probably due to a more uniform SiO_2 coating around the MCCII particles as described previously (*vide supra).* Prosolv® SMCC50 compacts were found to be the strongest followed by SD-CII:SiO_2 (95:5) and SD-CII:SiO_2 (90:10). On the contrary, SDCII and MCCII compacts showed the lowest tensile strength values. SD-CII:SiO_2 (80:20) and SD-CII:SiO_2 (98:2) showed values in between indicating that there is not a trend of reinforcement caused by silicification indicating that either a very high or very low levels are unfavorable for particle binding. The parameters derived from the Leuenberger model are shown in Table 5. The γ_c constant is related with the compressibility of the material. The higher the γ_c value, the faster the plateau in the curve is reached with increasing applied pressure. Highly plastic deforming materials, such as Prosolv® SMCC 50 exhibited the highest compression susceptibility value (0.006 MPa^{-1}), while the CII:SiO_2 composite brittle-like materials showed lower values (less than 0.005 MPa^{-1}). A plateau in the curve for Prosolv® SMCC 50 is reached sooner than those for the CII:SiO_2 composites. It is not surprising than the model predict higher maximum tensile strength (T_{max}) values for CII:SiO_2 composite materials at infinitive compression pressure (solid fraction of 1) since the increase in the amount of SiO_2 makes the rate of change of tensile strength with porosity and compression pressure slower and no plateau is seen in the range of pressures used.

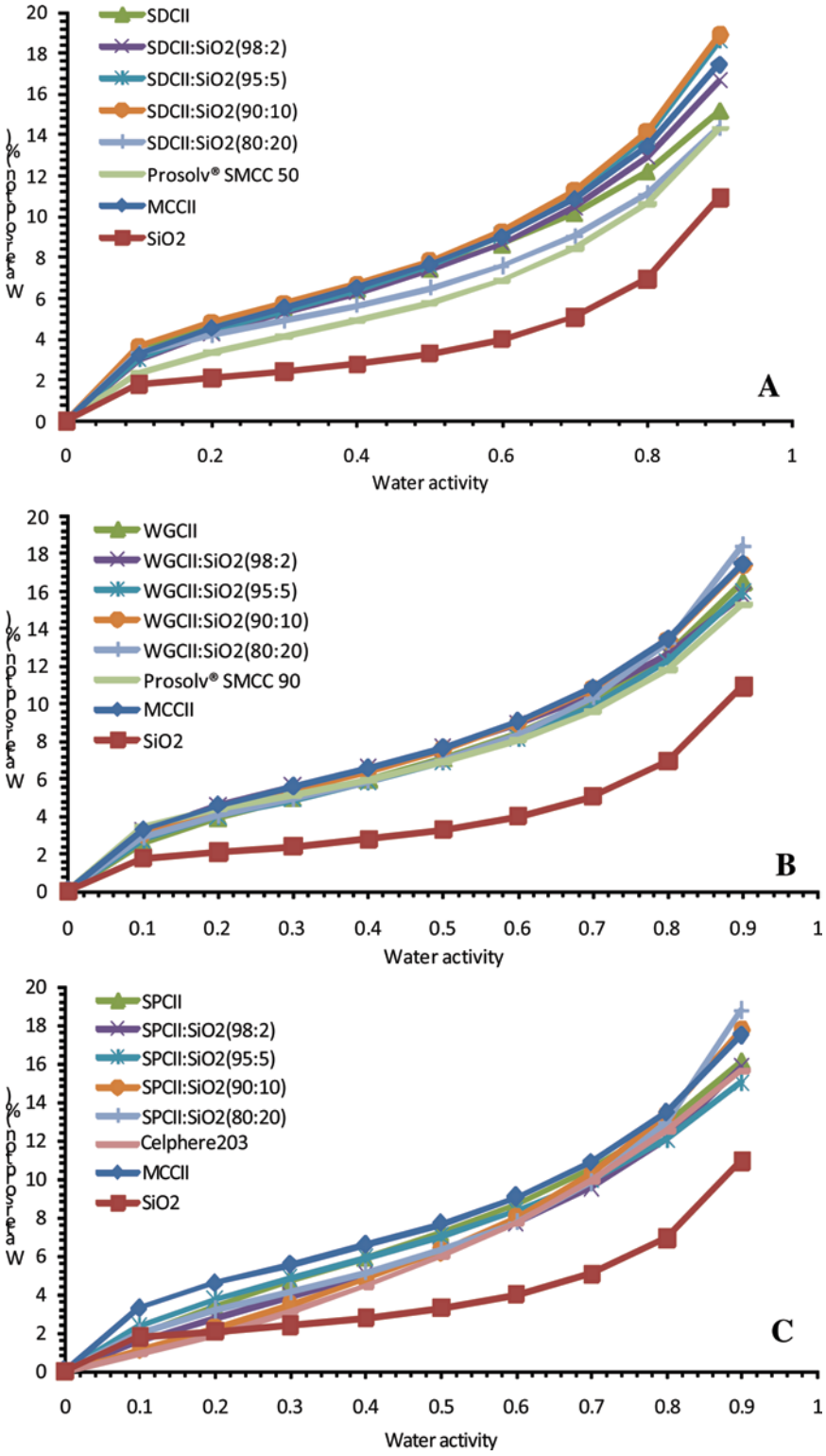

Figure 9. Fitted water sorption isotherms of the CII:SiO_2 composite according to the GAB model.

In the wet granulated materials a 10% silicification level rendered a material with the highest tensile strength (~7 MPa). However, these values were not as high as the one achieved by the SD-CII:SiO_2 (95:5) product (Figure 11). As seen before for the spray-dried materials, the theoretical maximum tensile strength (T_{max}) for the wet granulated materials increases as the amount of SiO_2 increases, being the highest for WG-CII:SiO_2(80:20). Compared to WG-CII, the compressibility parameter (γ_c) decreased as the level of silicification increased. In this case, the powder yield pressure increased as the level of silicification increased (given by a low γ_c). That ranged from 0.005 to 0.001 MPa^{-1} and from 0.004 to 0.001 MPa^{-1} for the spray-dried and wet granulated

Table 4. Hydrophilicity wetting and swelling properties of CII:SiO_2 composites ($n=3$).

Sample	m_m ±SD (g/g)	C ±SD	K ±SD	R^2	Swelling value (ml/g)	Contact angle (°)
MCCII	0.05 ± 0.00	16.9 ± 1.9	0.8 ± 0.0	0.9993	0.3 ± 0.1	0 ± 0
SD-CII	0.05 ± 0.00	21.3 ± 1.7	0.8 ± 0.0	0.9988	1.0 ± 0.1	0 ± 0
SD-CII:SiO_2(98:2)	0.05 ± 0.00	14.9 ± 0.6	0.8 ± 0.0	0.9993	0.9 ± 0.1	0 ± 0
SD-CII:SiO_2(95:5)	0.05 ± 0.00	14.9 ± 6.6	0.8 ± 0.0	0.9987	0.5 ± 0.1	0 ± 0
SD-CII:SiO_2 (90:10)	0.05 ± 0.06	24.3 ± 13.7	0.8 ± 0.1	0.9967	0.5 ± 0.1	0 ± 0
SD-CII:SiO_2 (80:20)	0.04 ± 0.00	35.6 ± 1.8	0.8 ± 0.0	0.9967	0.3 ± 0.1	0 ± 0
Prosolv® SMCC50	0.04 ± 0.00	15.8 ± 2.6	0.8 ± 0.0	0.9994	0.2 ± 0.1	23.6 ± 3.8
WG-CII	0.05 ± 0.00	11.3 ± 4.0	0.80 ± 0.0	0.9982	0.6 ± 0.0	0 ± 0
WG-CII: SiO_2 (98:2)	0.05 ± 0.00	15.5 ± 3.3	0.80 ± 0.0	0.9992	0.6 ± 0.1	0 ± 0
WG-CII: SiO_2 (95:5)	0.05 ± 0.01	13.6 ± 2.3	0.80 ± 0.0	0.9992	0.7 ± 0.1	0 ± 0
WG-CII: SiO_2 (90:10)	0.05 ± 0.01	14.4 ± 2.4	0.80 ± 0.0	0.9997	0.5 ± 0.1	0 ± 0
WG-CII:SiO_2 (80:20)	0.04 ± 0.01	16.8 ± 4.8	0.90 ± 0.0	0.9998	0.5 ± 0.1	0 ± 0
Prosolv® SMCC90	0.04 ± 0.00	29.9 ± 3.4	0.80 ± 0.0	0.9980	0.5 ± 0.2	23.6 ± 3.4
SPCII	0.06 ± 0.00	4.3 ± 1.7	0.7 ± 0.1	0.9960	0.7 ± 0.1	0 ± 0
SP-CII: SiO_2 (98:2)	0.05 ± 0.01	4.7 ± 0.8	0.8 ± 0.0	0.9968	0.6 ± 0.0	0 ± 0
SP-CII: SiO_2 (95:5)	0.06 ± 0.00	8.5 ± 5.9	0.7 ± 0.0	0.9961	0.7 ± 0.1	0 ± 0
SP-CII: SiO_2 (90:10)	0.06 ± 0.00	2.3 ± 0.8	0.8 ± 0.1	0.9967	0.6 ± 0.1	0 ± 0
SP-CII: SiO_2 (80:20)	0.04 ± 0.00	8.6 ± 0.1	0.9 ± 0.0	0.9998	0.6 ± 0.0	0 ± 0
Celphere203	0.15 ± 0.01	1.0 ± 0.1	0.6 ± 0.1	0.9897	0.6 ± 0.0	0 ± 0
SiO_2	0.02 ± 0.00	100.0 ± 0.0	0.9 ± 0.0	0.9842	0.0 ± 0.0	N.D.

M_m,monolayer capacity; c, monolayer energy constant; k, multilayer energy constant; °degrees; N.D., Not determined, it was not possible to make compacts.

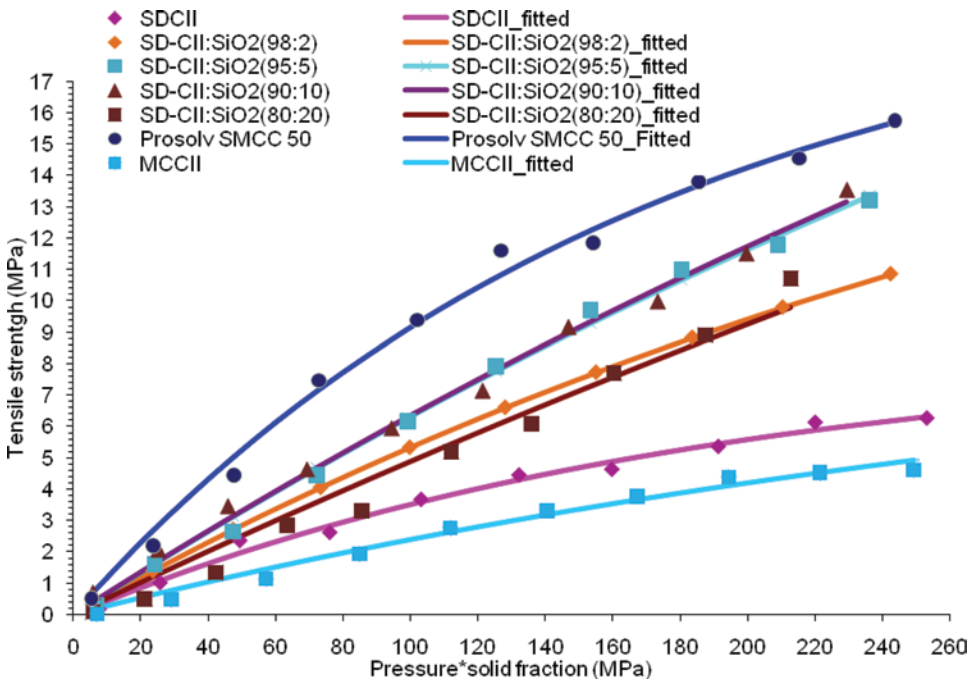

Figure 10. Effect of the SiO_2 content on the compactibility of MCCII according to the Leuenberger model for the spray dried materials.

materials, respectively. Conversely, Prosolv® SMCC50 and Prosolv® SMCC90 had high γ_c values (0.006 and 0.005, respectively). This indicates that these materials are more plastic deforming materials than CII:SiO_2 composites. The area under the curve of tensile strength of the spray-dried and wet granulated materials can be used to select a material for each process with the best mechanical properties. The rank observed for the spray dried materials was: Prosolv® SMCC 50>CII-SiO_2 (95:5)> CII-SiO_2 (90:10)> CII-SiO_2 (98:2)> CII-SiO_2 (80:20)>SD-CII>MCCII. Likewise the trend observed for the wet granulated materials was: Prosolv® SMCC90>WG-CII-SiO_2 (90:10)> WG-CII> WG-CII-SiO_2 (95:5)> WG-CII-SiO_2(98:2)> MCCII>CII-SiO_2 (80:20).

Compacts made from the CII:SiO_2 composites and Celphere203 were so weak that eroded and broke with handling and manipulation, independent of the compression force used and for this reason results were not included. This might be caused by the regular semi-spherical and smooth surface of the beads. These characteristics might limit the mechanical interlocking and formation of contact points needed for consolidation and particle binding under pressure. For this reason, the spheronized composite materials were rejected as the first choice for direct compression and hence, further studies of the mechanical properties of these materials was not attempted.

Table 5. Parameter derived from the Leuenberger the CII:SiO_2 composites.

Sample	AUCTS (MPa^2)	T_{max} (MPa)	γ_c (MPa^{-1})	R^2
MCCII	680.5	9.9	0.003	0.9835
SD-CII: SiO_2(80:20)	1082.5	47.0	0.001	0.9841
SD-CII: SiO_2(90:10)	1596.0	42.0	0.002	0.9937
SD-CII:SiO_2(95:5)	1683.2	40.0	0.002	0.9960
SD-CII:SiO_2(98:2)	1460.0	22.7	0.003	0.9924
SD-CII	969.0	8.5	0.005	0.9895
Prosolv® SMCC50	2348.7	20.7	0.006	0.9939
WG-CII: SiO_2(80:20)	632.7	51.8	0.001	0.9721
WG-CII: SiO_2(90:10)	1038.9	42.6	0.001	0.9769
WG-CII:SiO_2(95:5)	885.0	42.2	0.001	0.9890
WG-CII:SiO_2(98:2)	835.2	20.2	0.002	0.9627
WG-CII	1023.8	10.7	0.004	0.9835
Prosolv® SMCC90	2229.8	21.6	0.005	0.9986

Figure 12 shows that the fast disintegrating properties of MCCII were not affected by silicification or the spray-drying process, except for the SD-CII:SiO_2(80:20), which was lingered up to 120 sec at compression pressures of 260 MPa. On the contrary, Prosolv® SMCC50 up to compression pressures of 60 MPa presented a high disintegration value of 20 min; beyond this pressure compacts did not disintegrate during the test period (~300 min). Long disintegration times are expected for this material since it presented a high compactibility making it able to form strong compacts.

Figure 13 shows that compacts of the wet granulated composites disintegrated in less than 190 sec even the ones made at compression pressures as high as 260 MPa. On the contrary, compacts made of Prosolv® SMCC90 at 60 MPa disintegrated within 49 min. Beyond 60 MPa compacts did not disintegrate during the test period (~300 min). In general, the fast disintegrating property of MCCII is not affected by the level of silicification. These results are in agreement with those obtained for the spray-dried materials.

Conclusions

Morphological and powder characteristics of MCCII depended on silicification and process employed. Particle size, flow tap and bulk densities were the highest and porosity and Hausner ratio were the lowest for spheronized products followed by wet granulation and spray drying Independent of silicification level. On the contrary, properties such as true density, specific surface area and degree of crystallinity were more dependent on silicification rather than on processing. Degree

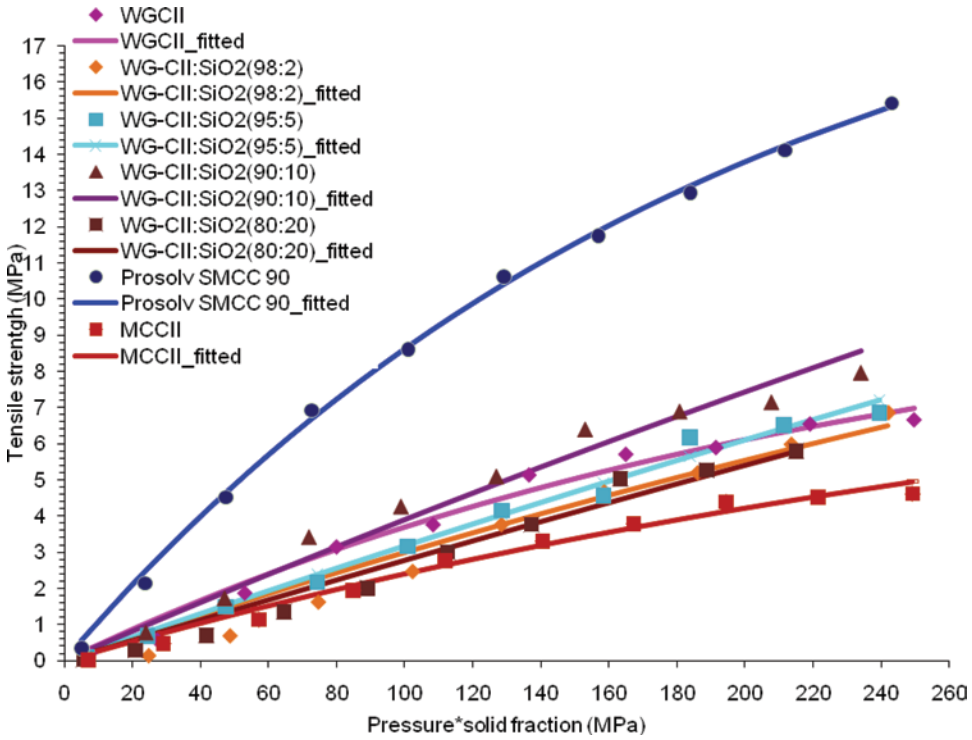

Figure 11. Effect of the SiO_2 content on the compactibility of MCCII according to the Leuenberger model for the wet granulated materials.

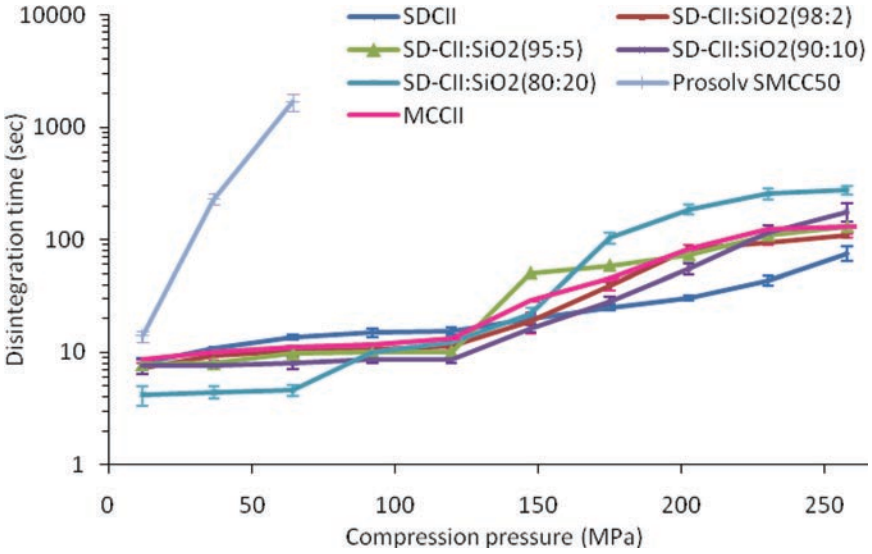

Figure 12. Effect of silicification on the disintegrating properties of the spray dried materials.

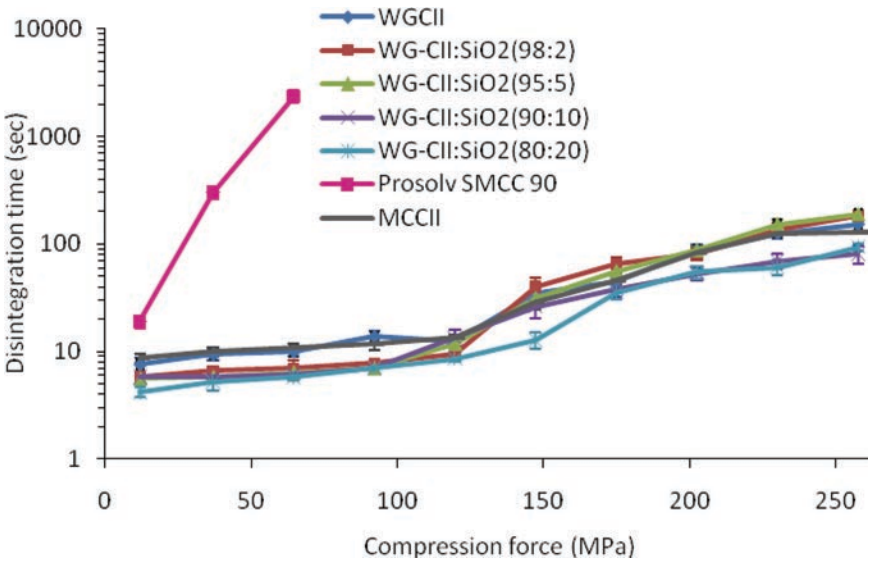

Figure 13. Effect of silicification on the disintegrating properties of the wet granulated materials.

of polymerization and moisture content were silicification and processing independent. Water sorption and swelling decreased at a 20% silicification independent of the process employed. Except for Celphere203, contact angles of cellulose I materials were higher than those of MCCII and CII:SiO_2 composites. A 5 and 10% silicification produced the strongest compacts for the spray dried and wet granulated materials. Opposite to Prosolvs, silicification did not affect the fast disintegrating properties of MCCII.

Acknowledgements

The authors thank The University of Antioquia for sponsoring the PhD studies of Mr. John Rojas. We also thank Jean Ross, Randy Nessler and Chantal Allmargot for their valuable critiques and training on the SEM and X-Ray microanalysis techniques.

Declaration of interest

The authors report no conflict of interest. The authors alone are responsible for the content of this paper.

References

1. Marwaha M, Sandhu D, Marwaha R. (2010). Coprocessing of excipients: A review on excipient development for improved tableting performance. Int J Appl Pharm, 2:41–47.
2. Díaz CC, Villafuerte L. (2010). Surrogate functionality of celluloses as tablet excipients Drug Dev. Ind. Pharm, 36:1422–1435.
3. Block LH, Moreton RC, Apte SP, Wendt RH, Munson EJ, Creekmore JR. (2009). Co-processed Excipients. Pharm forum, 35:1026–1028.
4. Reimerdes D. (1993).The near future of tablet excipients. Manuf Chem, 64:14–15.
5. Lerk C, Bolhuis G, De Boer A. (1974). Comparative evaluation of excipients for direct compression, II. Pharm Weekbl, 109:945–955.

6. Jain SP, Singh PP, Amin PD. (2010). Alternative extrusion-spheronization aids. Drug Dev Ind Pharm, 36:1364–1376.
7. Aljaberi A, Chatterji A, Shah NH, Sandhu HK. (2009). Functional performance of silicified microcrystalline cellulose versus microcrystalline cellulose: a case study. Drug Dev Ind Pharm, 35:1066–1071.
8. Nachaegari SK, Bansal AK. (2004). Coprocessed excipients for solid dosage forms. Pharm Technol, 28:52–65.
9. Chow K, Tong HH, Lum S, Chow AH. (2008). Engineering of pharmaceutical materials: an industrial perspective. j Pharm Sci, 97:2855–2877.
10. Kumar V, de la Luz Reus-Medina M, Yang D. (2002). Preparation, characterization, and tabletting properties of a new cellulose-based pharmaceutical aid. Int j Pharm, 235:129–140.
11. Reus M, Lenz M, Kumar V, Leuenberger H. (2004). Comparative Evaluation of Mechanical Properties of UICEL and Commercial Microcrystalline and Powdered Celluloses. J Pharm Pharmacol, 56:951–958.
12. M., Reus. Preparation, characterization and tableting properties of cellulose II powders. (2005). PhD Dissertation. The University of Iowa. Iowa City.
13. de la Luz Reus Medina M, Kumar V. (2006). Evaluation of cellulose II powders as a potential multifunctional excipient in tablet formulations. Int j Pharm, 322:31–35.
14. Van den Berg C. (1984). Description of water activity of foods for engineering purposes by means of the GAB model of sorption. Eng Food, 1:311–321.
15. Adamson A, Gast PG. (1997). Physical Chemistry of Surfaces. 6th ed. New York. Wiley-Interscience.
16. Edge S, Belu AM, Potter UJ, Steele DF, Young PM, Price R et al. (2002). Chemical characterisation of sodium starch glycolate particles. Int j Pharm, 240:67–78.
17. Edge S, Steele DF, Staniforth JN, Chen A, Woodcock PM. (2002). Powder compaction properties of sodium starch glycolate disintegrants. Drug Dev Ind Pharm, 28:989–999.
18. Fell JT, Newton JM. (1968). The tensile strength of lactose tablets. j Pharm Pharmacol, 20:657–659.
19. Lanz M. (2005). Pharmaceutical powder technology: Towards a science based understanding of the behavior of powder systems. Basel: University of Basel. PhD dissertation, 1–162.
20. Klemm D, Philipp B, Heinze T, Heinze U. (1998). Comprehensive Cellulose Chemistry: Functionalization of Cellulose. New York. John Wiley & sons.
21. Kothari SH, Kumar V, Banker GS. (2002). Comparative evaluations of powder and mechanical properties of low crystallinity celluloses, microcrystalline celluloses, and powdered celluloses. Int j Pharm, 232:69–80.
22. Tobyn MJ, McCarthy GP, Staniforth JN, Edge S. (1998). Physicochemical comparison between microcrystalline cellulose and silicified microcrystalline cellulose. Int J Pharm, 169:183–194.
23. Edge S, Steele FD, Tobyn M, Staniforth JN. (1999). Polysacharide engineering: Silicified microcrystalline cellulose as a novel high-functionality pharmaceutical material in: ACS Symposium series # 737: Polysacharadides applications: cosmetics and pharmaceuticals. American Chemical Society. Washington D.C. 368–376.
24. Portmann C, Ziolko T, Wiprachtiger A, Kleinhan S, Schonenberger G. (2007). The Laboratory Assistant. Switzerland. Buchi Labortechnik.
25. Cabot. CAB-O-SIL Fume silica properties and functions. Cabot (1987). CGen-8:1–36.
26. Zhang Y, Law Y, Chakrabarti S. (2003). Physical properties and compact analysis of commonly used direct compression binders. aaps Pharmscitech, 4:E62.